Check for updates

Influence of Accident-Tolerant Fuel With Steel Cladding for Sustainable Heat Transfer in the Reactor Core of VVER-1200

MD Tanzib Ehsan Sanglap
Department of Theoretical and Experimental Physics of Nuclear Reactors,
National Research Nuclear University MEPhI (Moscow Engineering Physics Institute),
Kashirskaya Highway, 31,
Moscow 115409, Russia
e-mail: tanzibehsan@iut-dhaka.edu

Sazidur Rahman Shahriar[1]
Department of Mechanical Engineering,
Prairie View A&M University,
100 University Drive,
Prairie View, TX 77446
e-mail: sshahriar@pvamu.edu

Since the events at the Fukushima–Daiichi nuclear power plant, there has been increased interest in developing accident tolerant fuel (ATF) to avoid accidents for light water reactors where Uranium-Silicide-based fuel has an excellent field to minimize the hydrogen hazards. Similarly, steel cladding is at the center of attraction for researchers nowadays. In this research, the feasibility of using Uranium-Silicides (i.e., U_3Si, U_3Si_2, and U_3Si_5) combined with different types of austenitic steel (i.e., AISI) was investigated to improve the safety performance. A three-dimensional (3D) computational fluid dynamics (CFD)-coded STAR CCM+ model was used to assess heat transfer performance in the hexagonal fuel assembly of a supercritical water-cooled reactor VVER-1200. Utilizing the computational environment of STAR CCM+, the test analysis was conducted for a portion of fuel height using the realizable K-Epsilon Two-Layer Wall turbulence model. This analysis showed that the combination of U_3Si_2 fuel with AISI-348 cladding got superiority over other ATF-AISI fuel-claddings assemblies to use in the reactor core of VVER-1200 because of their lower central fuel temperature value with good mechanical and thermal advantages. This work also derived an empirical heat transfer coefficient equation to guide the relevant future investigations on the thermal analysis of the core.
[DOI: 10.1115/1.4054476]

Keywords: clean energy, computational fluid dynamics (CFD), current reactors, heat transfer, nuclear fuels and materials, nuclear safety and security, simulation and design, sustainability, thermal analysis

Downloaded from http://risk.asmedigitalcollection.asme.org/openengineering/article-pdf/doi/10.1115/1.4054476/6881352/aoje_1_011023.pdf by guest on 23 June 2024

1 Introduction

The nuclear fuel system of all light water reactors (LWRs) worldwide is currently based on the combination of slightly enriched UO_2 pellets confined in Zirconium-alloy-based fuel-cladding. In March 2011, a magnitude of 9.0-grade earthquake occurred in Japan's coastal area, causing a tsunami in that area [1]. The cost of this occurrence was more than hundreds of million dollars [2]. The tsunami results in a surge flooding in the backup power generator rooms at the Fukushima–Daiichi in Nuclear Power Plants (NPP). The loss of power to coolant systems leads to high temperatures, oxidation of Zr-based alloys, hydrogen production, melted fuel, and hydrogen explosions.

Moreover, during the loss of coolant in the core when the cladding is exposed to high-temperature steam, Zr alloys experience exothermic oxidation, which accelerates the progression of an accident, and the core may meltdown [3]. The economic impacts, both directly related to the clean-up and those generally affecting the nuclear energy sector, are significant [4].

The hydrogen production phenomenon was described by A.R. Massih [5], indicating the margin of safety to withstand hydrogen production, which causes cladding failure (i.e., cracking, melting, and cladding degradation) at high temperatures. Moreover, if any breakdown in any zone of fuel-cladding occurs, then water and steam go in touch with the UO_2. So, it oxidized and caused the production of hydrogen.

$$Zr + 2H_2O \overset{800\,^{\circ}C}{\rightarrow} ZrO_2 + 2H_2$$

The oxidation of UO_2 fuel under normal and abnormal to severe accidental conditions occurs when fuel-cladding fails caused by using Zirconium as cladding material by specific characteristics based on their design specifications. The radiation exposure probability is highest as soon as the meltdown scenario starts. So, an alternative way of using Uranium needed to be checked to avoid any other circumstances. In this regard, many researchers sought an excellent Silicide as a perfect option to compete with conventional fuel for securing safety and lowering hydrogen production in NPPs. However, the thermal stability within its melting points (Tables 1 and 7) is the major challenge which is a disadvantage of ura-silicides and steel cladding, whereas UO_2 and Zr are 2840 °C, and 1825 °C, respectively. But to improve tolerance of loss of cooling accidents (LOCA) in current reactor systems, modern reactor technology urge a new fuel system with improved fuel and cladding behaviors at high fuel temperatures, against hydrogen generation, fission product release, and fuel melting [6].

Moreover, Bischoffs [7] and his team developed a fuel concept of accident tolerant fuel (ATF) and related properties to be considered during fuel development such as melting temperature, thermal conductivity, oxidation reaction kinetics with high-temperature steam to reduce the heat and hydrogen production, and fuel thermo-mechanical properties to maintain cool able geometry at high-temperature fuel pellet.

Hence, this research aims to identify the best ATF combination which can generate high temperature but in the margin of its melting point using STAR CCM+. Moreover, categorizing and integrating different heat transfer coefficient (HTC) equations, another objective of this article is to state a simple HTC equation along with the height of the core.

1.1 U_xSi_x as Fuel Material.

The information about Uranium–Silicide pellets was investigated by many researchers in different

[1]Corresponding author.

Manuscript received October 19, 2021; final manuscript received April 26, 2022; published online May 17, 2022. Assoc. Editor: Emmanuel Porcheron.

Copyright © 2022 by ASME

Table 1 Thermal properties of austenitic stainless steels

AISI	Melting point (°C)	Conductivity (W $m^{-1}K^{-1}$)	Expansion (10^{-6} K)
304	1433	16.3	16.6
310	1466	14.2	16
316	1427	15.9	16–18
347	1425	16.3	16–18
348	1443	19.1	18.5

branches of science. The U–Si compounds varied in different forms, such as U_3Si_2, U_3Si, U–Si, and U_3Si_5. Its (U–Si) thermal conductivity is higher than that of uranium dioxide at operating temperatures where Uranium dioxide's thermal conductivity decreases as a function of temperature [8,9]. This thermal conductivity offsets its melting point (2865 °C), such that the fuel is operating and has safety margins.

In this regard, White et al. [10–12] identified that U_3Si_5 and U_3Si_2 have similar onset oxidation temperatures, whereas the oxidation of U_3Si_2 is faster. Moreover, U_3Si_2 is recognized as a better option, because of its higher resistance to irradiation-induced macroscopic swelling and amorphization [13–16].

Antonia and Gofryka calculated the thermal conductivity of U_3Si_2 in the temperature range of 2–300 K, and magnetic fields up to 9 T were about 8.5 W/m-K at 300 K, which was idealized by electronic and lattice contributions. In this case, the lattice part of the total thermal conductivity was relatively minor in U_3Si [17].

Besides, U_3Si_5 has a lower U density (7.5 gU/cm^3) than U_3Si (14.8 gU/cm^3) and U_3Si (12.2 gU/cm^3), causing a higher melting point (1770 °C) than those of U_3Si (925 °C) and U_3Si_2 (1665 °C). Under the oxidizing atmosphere at rising temperatures at 1500 °C, U_3Si_5 was suspected as less susceptible to rapid oxidative pulverization temperatures at which the samples are fragmented [10–12,18]. Based on the analysis, U_3Si_2 will remain crystalline without complete amorphization above ~230–330 °C, the temperatures relevant to the LWR reactor operations [19]. Moreover, U_3Si_2 as an LWR fuel requires satisfactory thermal performance across 22 areas [20].

Besides, the Uranium density of U_3Si_5 with a lower U/Si ratio of 0.58 also suggests that the use of such fuel could be broadly envisioned if a higher U was allowed for specialty reactor designs or as a second fissile phase in a composite fuel [11]. Chen and Yuan [21] also suggested that U_3Si_2 fuel is an excellent candidate for ATF due to its high thermal conductivity and high Uranium density. It also transfers heat four times faster, allowing the fuel to last longer in accident conditions [22].

1.2 Austenitic Steel as a Cladding Material. In nuclear reactors, the use of steel as fuel-cladding material has some advantages such as (i) good mechanical and (ii) corrosion resistance [23,24]. But during a loss-of-coolant accident, the main benefit is signified as reducing the amount of hydrogen released.

Moreover, steel 304 was used as a cladding material in the first pressurized water reactor (PWR) with a good performance in the 1960s. Then, alternated cladding materials such as alloys (AISI-304, AISI-310, AISI-316, and AISI-347) were checked to realize their performance and safety [25]. The mechanical properties of austenitic steel were also analyzed by Chawla [23], Beeston [26], Peckner and Berstein [27], and Pasupathi [28], which are combined in Table 1.

Furthermore, the elastic modulus of 348 is higher than Zircaloy-4, which means that the cladding deformation is much smaller than those of Zircaloy-4 cladding. This behavior was confirmed using simulations carried out using adapted fuel performance codes to evaluate fuel rods with AISI 348 as cladding and comparing to the performance of Zircaloy-4 under a common power history [24,29].

In the reactor core, the cladding material should have a high tensile strength [30], and the tensile strength of AISI 348 is highest at 655 MPa. According to Beston's analysis, considering its other mechanical properties is also an intolerable range. Thus, the AISI 348 would be a good choice. The early investigation found that irradiation of PWR is operated for a period using annealed 348 as cladding, confirming its good performance [31]. Moreover, the void formation probability in AISI steel cladding is lower due to the neutron fragments when irradiated in a fast neutron flux at a higher temperature (more than 650 °C). Since 1960, stainless steel as a cladding material has allowed PWR efficiency due to the lower absorption cross-section of thermal neutrons [24]. Considering such potential aspects, this research investigates steel's thermal characteristics as cladding materials with the ATF.

1.3 Heat Transfer Coefficient Equation. The HTC equations from several renowned researchers are well categorized for checking the sustainable heat transfer in the tables (Tables 2 and 3). In this analysis, correlations were implemented, and their prediction capabilities of heat transfer for supercritical water and HTCs need to be assessed.

Integrating frictional factors, the developed correlation equations for heat transfer in supercritical fluids have been developed by Russian researchers Petukhov et al. [32] and Krasnoshchekov Protopopov [33], where the factors of the tube or surface are under consideration. The correlations and conditions are listed in Table 3, which uses various HTC applications.

2 Materials and Methods

The theoretical calculation of the average and surface temperature of the fuel was needed to identify the maximum temperature

Table 2 Heat transfer correlations derived from the Dittus–Boelter equation

Eqn. No.	References	Correlations	Flow Geometry
(1)	Dittus and Boelter [37]	$Nu_b = 0.025\ Re_b^{0.8} Pr_b^{0.4}$	For the case of heating the tube
(2)	Griem [38]	$Nu_b = 0.0169\ Re_b^{0.8356} Pr_b^{0.432}$	Tubes
(3)	Shitsman [41]	$Nu_b = 0.023\ Pr_{min}^{0.8} Re_b^{0.8}$	Tubes ($D = 7.8$, 8.2 mm)
(4)	Dwyer [42]	$Nu = 6.66 + 3.126\left(\frac{S}{D}\right) + 1.184\left(\frac{S}{D}\right)^2 + 0.0155(\psi Pe)^{0.86}$	S = distance between two fuel rod pitch D = fuel diameter
(5)	Kalinin and Dreitser [39]	$Nu = (0.032X - 0.0144)Re^{0.8}\ Pr^{\frac{1}{3}}$; Here $X = \frac{S}{D}$	For bundle fuel rod
(6)	Churchill, and Bernstein [43]	$Nu = 0.3 + \frac{0.62\ Re^{0.5}\ Pr^{\frac{1}{3}}}{\left[1 + \left(\frac{0.4}{Pr}\right)^{\frac{2}{3}}\right]^{\frac{1}{4}}} \left[1 + \left(\frac{Re}{282{,}000}\right)^{\frac{5}{8}}\right]^{\frac{4}{5}}$	Cylindrical fuel rod (for Pr.Re ≥ 0.2)

Downloaded from http://risk.asmedigitalcollection.asme.org/openengineering/article-pdf/doi/10.1115/1.4054476/6881352/aoje_1_011023.pdf by guest on 23 June 2024

Table 3 Heat transfer correlations with frictional factor

Eqn No.	References	Correlations	Flow Geometry
(7)	Petukhov [32]	$\mathrm{Nu} = \dfrac{\frac{\zeta}{8}\,\mathrm{Re.Pr}}{\frac{900}{\mathrm{Re}} + K + 12.7\sqrt{\frac{\zeta}{8}}(\mathrm{Pr}^{2/3} - 1)}$ Here, $\zeta = (1.82\log(\mathrm{Re}) - 1.64)^{-2}$ and $K = 1 + \frac{900}{\mathrm{Re}}$	Tubes, upward, downward, and horizontal ($D = 10$ mm, $L = 3.67$ m
(8)	Gnielinski [40]	$\mathrm{Nu} = \dfrac{\frac{f}{8}(\mathrm{Re} - 1000)\mathrm{Pr}}{1 + 12.7\left(\frac{f}{8}\right)^{0.5}\left(\mathrm{Pr}^{\frac{2}{3}} - 1\right)}$ Here, $f = [0.79\ln(\mathrm{Re}) - 1.64]^{-2}$	Tubes, upward, downward, and horizontal ($D = 15$ mm, $L = 4.29$ m
(9)	Krasnoshchekov Protopopov [33]	$\mathrm{Nu}_o = \dfrac{\frac{\zeta}{8}\,\mathrm{Re.Pr}}{1.07 + 12.7\sqrt{\frac{\zeta}{8}}(\mathrm{Pr}^{2/3} - 1)}$ where $\zeta = (1.82\log(\mathrm{Re}) - 1.64)^2$	Tubes ($D = 1.6$–20 mm)

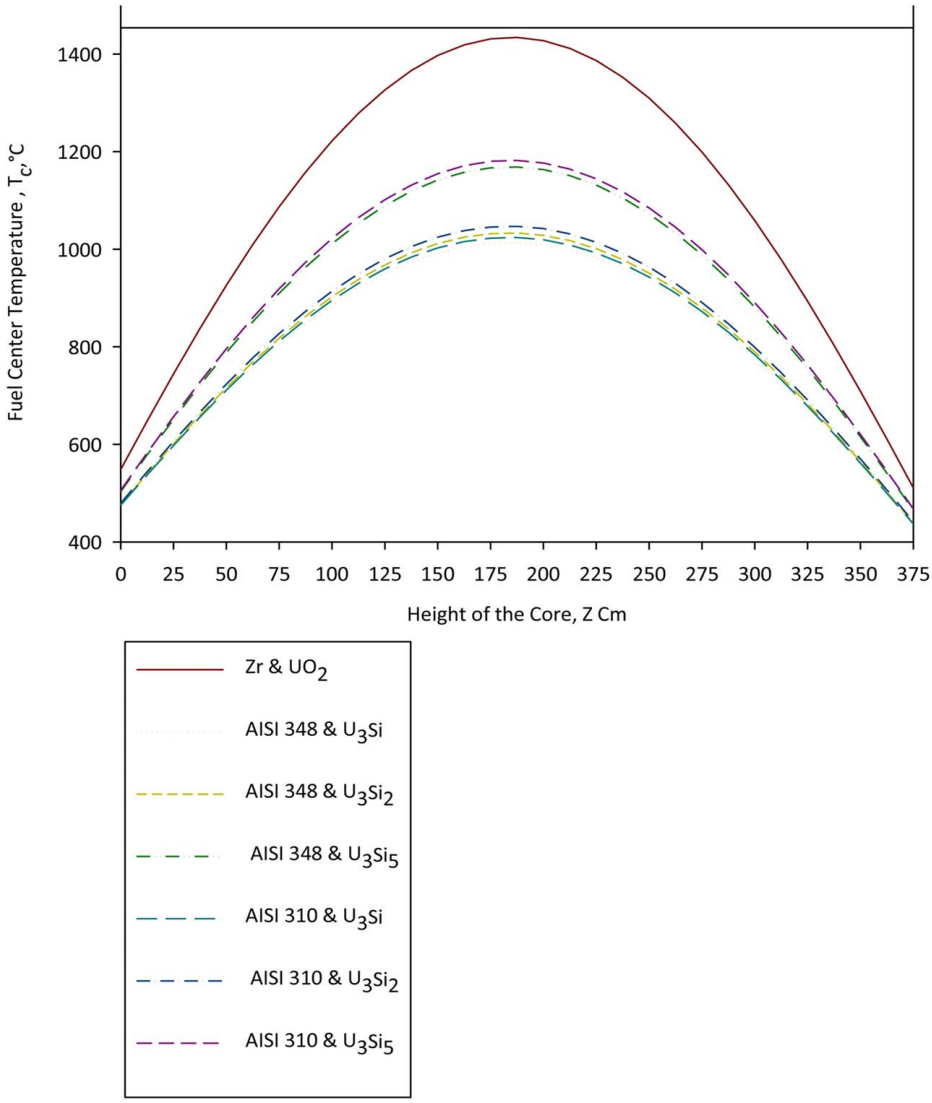

Fig. 1 Temperature distribution at the center of different fuel pellets depends on the coordinate of the height of the core for different cladding material and fuel material combinations

Downloaded from http://risk.asmedigitalcollection.asme.org/openengineering/article-pdf/doi/10.1115/1.4054476/6881352/aoje_1_011023.pdf by guest on 23 June 2024

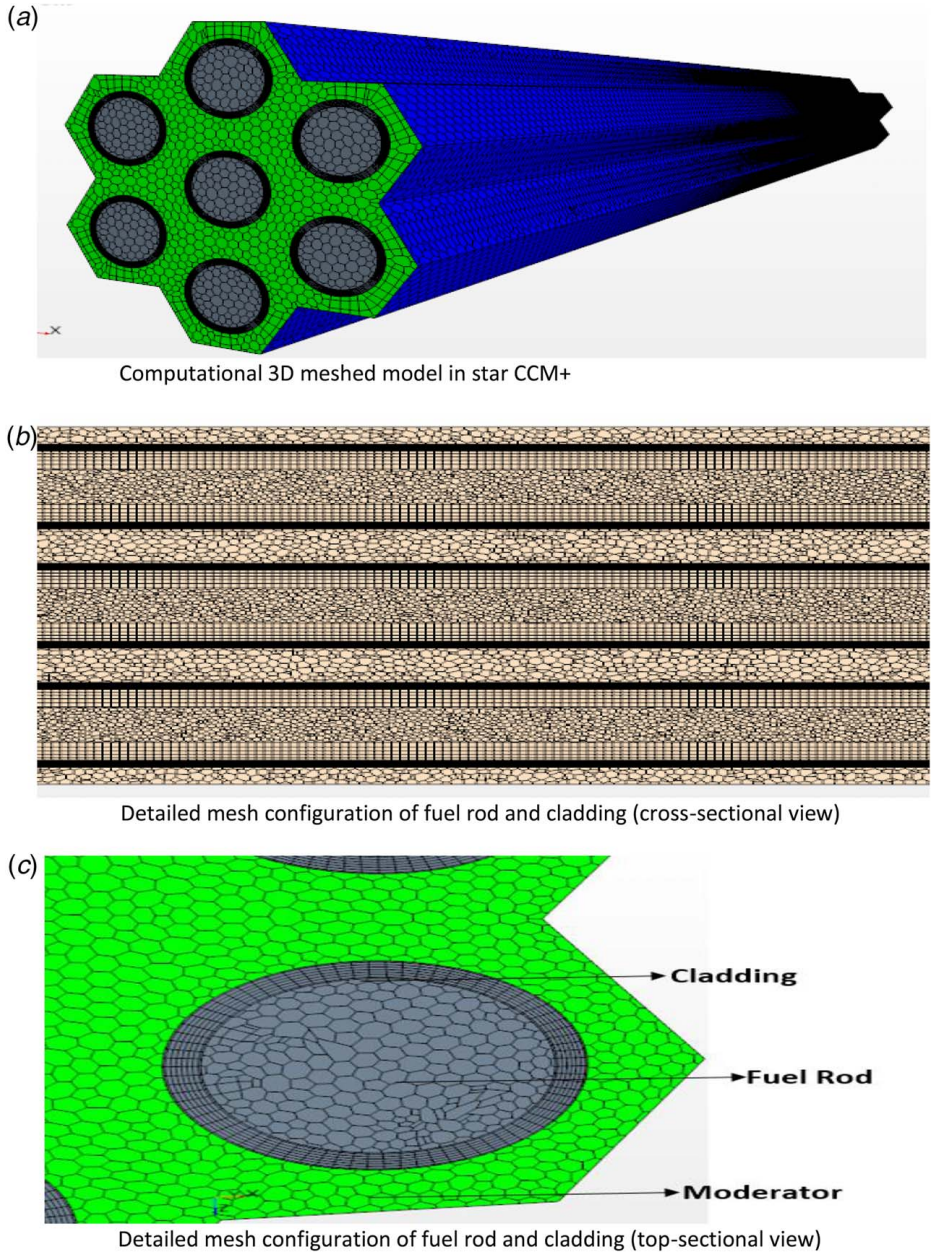

Fig. 2 (*a*) Computational 3D meshed model in STAR CCM+, (*b*) detailed mesh configuration of fuel rod and cladding (cross-sectional view), and (*c*) detailed mesh configuration of fuel rod and cladding (top-sectional view)

trends to give the proper justification for using a specific combination of fuel and cladding. The model in STAR CCM+ was developed for 30 cm, which needs to be verified by the theoretically calculated results. Similar characteristics (i.e., cladding temperature) between the simulated and theoretical data were found in the earlier investigation. The recommendation for fuel-cladding combinations and empirical HTC equation needs to be formulated for the first half of the uniform full-size core.

2.1 Fuel Center Temperature Distribution of Different Accident Tolerant Fuels. The conductivity of Uranium Carbide, Uranium Nitride (UN), and Uranium Silicide (U_3Si_2) are appreciably higher than that of UO_2 and increases with temperature rather than decreases. High thermal conductivity will reduce the centerline temperature to avoid melting the pellets and claddings. These theories justified the acquired results in this work were explained in STAR CCM+ by these theories.

To compare the ATF with conventional fuel, thermal distribution is one of the main parameters of this work. The comparison of temperature distribution of ATFs with conventional fuel in the center of the fuel pellet depending on the coordinate of the height of the core has been observed. Furthermore, according to Goldberg [34] and Rahgoshay and Rahmani [35], the total length of the reactor is 375 cms.

Table 4 Initial conditions

Initial turbulence intensity	0.01
Initial turbulent viscosity ratio	10.0
Turbulence velocity	1 m/s
Pressure	0 Pa
Static temperature	315 °C
Initial inlet temperature	330 °C
Initial avg. the temperature of the wall surface	470.656 °C

Downloaded from http://risk.asmedigitalcollection.asme.org/openengineering/article-pdf/doi/10.1115/1.4054476/6881352/aoje_1_011023.pdf by guest on 23 June 2024

Table 5 Specification of the model in STAR CCM+

Specification	Value
Number of the fuel rod	7 Psc.
Fuel rod material	$U_3SI/U_3Si_2/U_3Si_5/UO_2$
Number of cladding	7 Psc.
Cladding material	*AISI 310/348/Zr*
Pressure	16.2 MPa
Moderator	*Water (properties ref. IAPWS-IF97)*
Inlet temperature	298.2 °C
Total number of matrix cells	6 401 947
Constant field functions	
Mass flowrate	2.31 kg/s
Effective height	4.299 m
Fuel length	3.75 m
Assembly number	163
Number of fuel rods	312
Total thermal power	3212 MW
Pellet diameter	7.6 mm
Contact thermal resistance	3.2×10^{-4} m^2k/w
Configuration for mesh generators	
Surface re-mesher	
Size of the surface cells	0.6 mm
The minimum size of the surface cells	0.24
Surface growth rate	1.2
Parallel messer	*For cladding base size* (8 mm)
Polyhedral Mesher (without cladding)	*Base size* 12 mm
Number of prism layers	8
Prism layer stretching	1.2
The total thickness of the prism layer	9.6 mm
The flow and heat transfer model	
Three dimensional	*RANS* Turbulence model
Realizable k-epsilon two-layer wall treatment (2nd order gradient)	Segregated Fluid Temperature (Convection second-order modeling).
The heat transfer model for cladding and fuel pellet	
Three dimensional	Steady
Segregated solid energy	Constantan density

The distribution of T_c, with the T_{sh} and the height and the T_{avg} of fuel, was calculated every 5 cm. However, the temperature of coolant and cladding was previously calculated where no significant dependency on fuel height was found.

Moreover, to draw the periphery temperatures, $T_w(z)$ distribution, and the fuel resistance effect $R_f = 0$ in the following equation:

$$T_c(z) = T_{sh}(z) + q_o \cos\left(\frac{\pi z}{H_{eff}}\right)(R_{sh} + R_g + R_f)$$

Thus, the average temperature distribution at each point between the fuel center and the surface becomes

$$T_{avg}(z) = \frac{T_c(z) + T_w(z)}{2}$$

In this case, T_c equations correlates with Goldberg's theories. However, the fuel's center temperature varies due to thermal resistance and conductivity. Hence, an increase in thermal conductivity will reduce the melting point of each fuel. However, the distribution with the height needs to be clarified within the melting margin. Furthermore, the thermal distribution to use ATF compared to conventional fuel and cladding will be investigated based on the theoretically calculated and found a symmetric distribution as in Fig. 1.

2.2 Specification of the Model. In this analysis, the dimensions used for the model were obtained from an extract of the hexagonal fuel assembly configuration design. The overall computational meshed 3D model output from STAR CCM+ is visualized in Figs. 2(*a*)–2(*c*).

Prism layer meshes and surface re-meshes were applied with 16,401,947 small matrices or the modeling procedure to get a more accurate model for collecting basic information. The model was validated between temperature ranges 0 °C–5000 °C. Other specifications of the setting of the analytical model and flow and new heat transfer model of computational fluid dynamics (CFD) are prolonged in Tables 4 and 5, respectively.

In the heat transfer model, two-equation assumes that the turbulent fluctuations are locally isotropic with smaller eddies and high Reynolds. Moreover, the production and dissipation terms in the *k*-equation were considered for the localized heat equilibrium assumption for turbulence modeling. The finite element analytical model requires sophisticated facilities to integrate the gas gap. Hence, the contact resistance between the fuel pellet and the inner cladding surface was set as the gap conductance value of 3.2×10^{-44} to improve computational flexibility.

2.3 Boundary Conditions. The gradients were deployed using Green–Gauss/Weighted-Least-Squares Hybrid Gradient [36]. The symmetric non-slip boundary flow condition for the moderator took into account the intermolecular force and dragged between the fuel surface and the water moderator. Furthermore, the blended wall function values (rate of dissipation = 9.0, turbulence kinetic energy = 0.42) were chosen. They combined the moderator two-layer techniques with the usage of the function and resulted in a smoother transition flow. The constant mass flowrate of 2.31 kg/s was considered for the effective height of the models through the inlet to the outlet. According to the current VVER-1200 data references, all relevant values have been chosen without the wall configuration.

2.4 Model Evaluation. For evaluating the model, T_{avg} and T_c for Zircaloy 4 cladding and UO_2 fuel were also calculated and analyzed the similarity of the result to validate the model. In this regard, T_c and T_{avg} in minor errors which might occur due to the unavoidable assumptions (i.e., wall configuration, hydrogen gap). In Figs. 3(*a*) and 3(*b*) and Table 6, the variation in average temperature by theoretical and simulated value is observed. The average error was only 1.975% for T_{avg} distribution and 0.96% error for T_c distribution which validate the model for further analysis. Moreover, a

Table 6 Average temperature of the fuel for overall 30 cm of the fuel

Combination	Average theoretically calculated T_c°C	Average simulated T_c°C	T_c error %	Average theoretically calculated T_{av},°C	Average simulated T_{av},°C	T_{avg} error %
Zircaloy cladding and UO_2 fuel	555.61	560.64	0.91	492.73	483.00	1.97
AISI 348 cladding and U_3Si fuel	468.49	465.29	0.68	453.98	446.14	1.72
AISI 348 cladding and U_3Si_2 fuel	473.21	469.85	0.71	455.74	447.68	1.76
AISI 348 cladding and U_3Si_5 fuel	506.18	509.50	0.66	472.22	464.56	1.62
AISI 310 cladding and U_3Si fuel	471.86	473.17	0.28	456.75	447.97	1.92
AISI 310 cladding and U_3Si_2 fuel	476.58	479.72	0.66	459.10	451.43	1.67
AISI 310 cladding and U_3Si_5 fuel	509.52	511.82	0.45	475.58	467.60	1.68

Downloaded from http://risk.asmedigitalcollection.asme.org/openengineering/article-pdf/doi/10.1115/1.4054476/6881352/aoje_1_011023.pdf by guest on 23 June 2024

Table 7 Comparable thermal characteristics analysis for declaration

Fuel type	Melting point of the fuel, °C	Cladding type	The melting point of the cladding, °C	Simulated maximum, T_c °C (for 30 cm)	Theoretically calculated maximum T_c, °C (for full size)
U_3Si	925	AISI 348	1443	465.29	1010.70
		AISI 310	1466	473.17	1023.91
U_3Si_5	1775	AISI 348	1443	509.66	1167.46
		AISI 310	1466	515.98	1181.11

similar approach was also made for all other combinations by validating and then investigating all along ways of this research to justify the model at each stage in Table 6.

3 Results and Analysis

The thermal analysis revealed the best combination of U–Si and steel cladding considering fuel center temperature within each margin of melting point and a simple HTC equation along with the height of the core.

3.1 Fuel-Cladding Combination. In Figs. 4(*a*) and 4(*b*), the simulated data are graphically compared between different

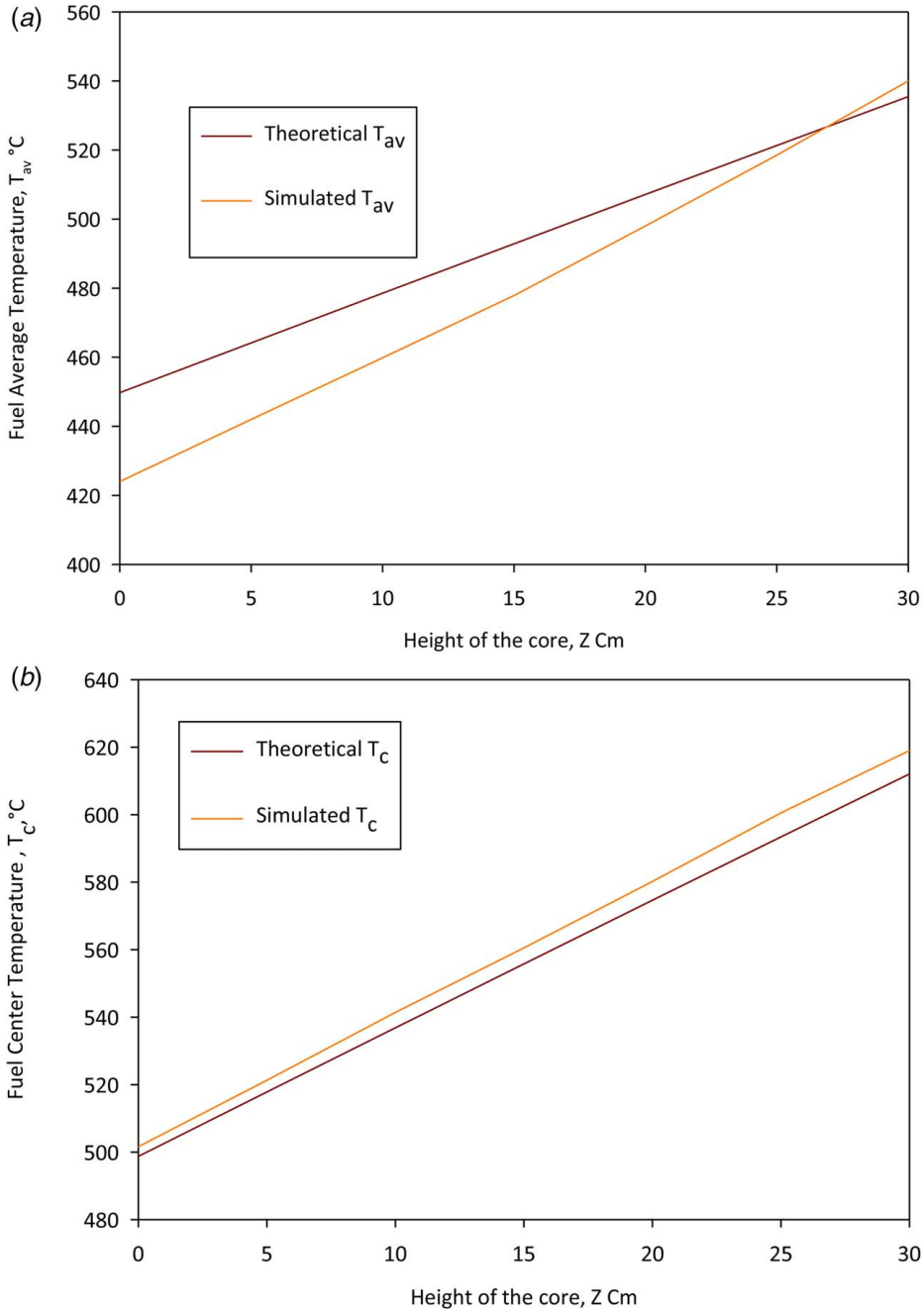

Fig. 3 (*a*) Average fuel temperature comparison for Zircaloy-4 cladding and UO_2 fuel and (*b*) center fuel temperature comparison for Zircaloy-4 cladding and UO_2 fuel

Downloaded from http://risk.asmedigitalcollection.asme.org/openengineering/article-pdf/doi/10.1115/1.4054476/6881352/aoje_1_011023.pdf by guest on 23 June 2024

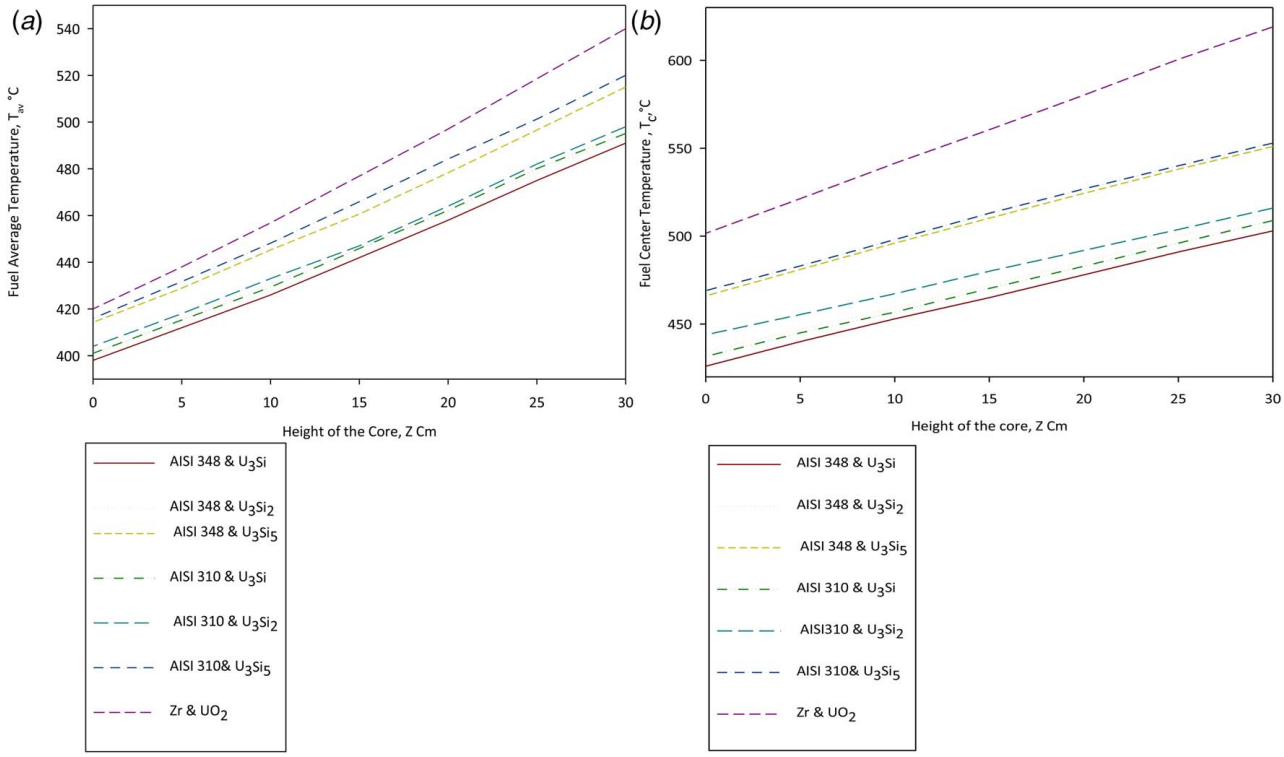

Fig. 4 (*a*) Fuel average temperature (T_{avg}) comparison between different fuel and cladding combinations and (*b*) Fuel maximum temperature (T_c) comparison between different fuel and cladding combination

combinations of fuel and cladding. Here, the analytical understanding from the turbulence model is that maximum T_{avg} and T_c for all varieties of ATF fuel-cladding are much lower than the conventional VVER-1200. Comparatively, the dependency on cladding type is slightly lower than the fuel. To expatiate the results, the overall average values are also mentioned for the first 30 cm of the fuel rod for different fuel-cladding material combinations in Table 6, which reassures the validation of the model and theoretical calculation and enable this research to state the best type of fuel combination calculation of full-size reactor from Fig. 1.

Furthermore, comparing all the combinations, U_3Si_2 fuel with AISI 348 anAISI 348 cladding and U_3Si_2 fuel got the i_2 fuel got third lowest T_c (1033.6 °C), which is within its melting margin. Among all other combinations, U_3Si_5 fuel and AISI 310, 348 cladding got a priority for reactor application for its higher T_c with high heat generation capabilities but within the melting limit (1775 °C). Precise indication has been noted in Table 7 properly comparing two sample combinations with the highest and lowest T_c.

However, for U_3Si fuel, the fuel maximum temperature T_c is higher than its melting point. Thus, it will cause reactor failure even during normal operating conditions; hence U_3Si, with any other cladding, should not apply to any reactor applications.

Moreover, earlier studies found that AISI 348 got higher mechanical and expansion advantages. Additionally, according to the

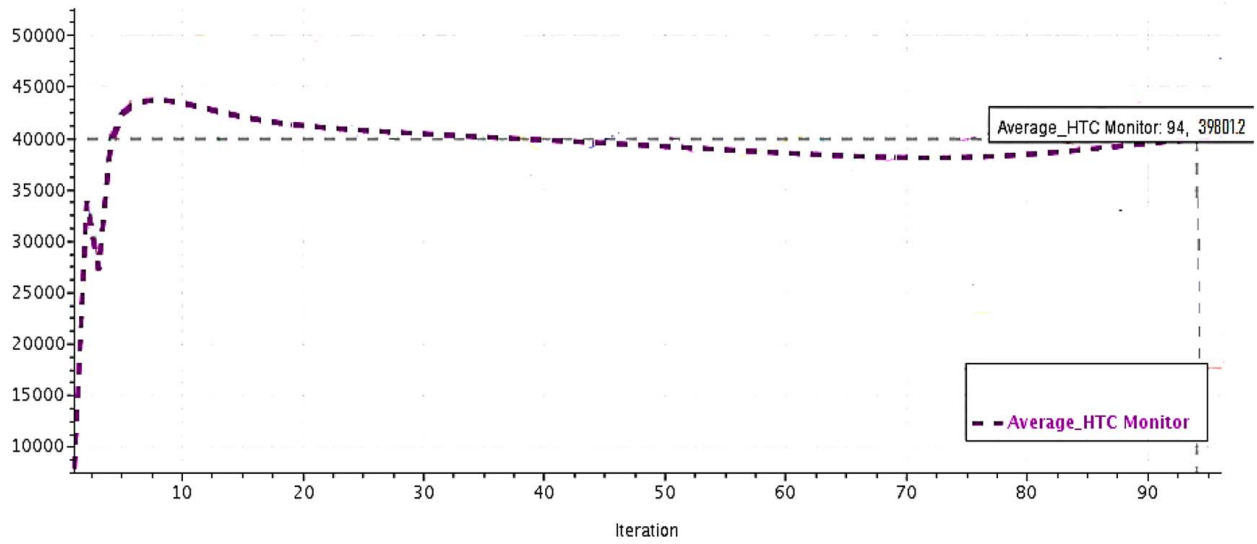

Fig. 5 Average HTC monitor plot in STAR CCM+

Downloaded from http://risk.asmedigitalcollection.asme.org/openengineering/article-pdf/doi/10.1115/1.4054476/6881352/aoje_1_011023.pdf by guest on 23 June 2024

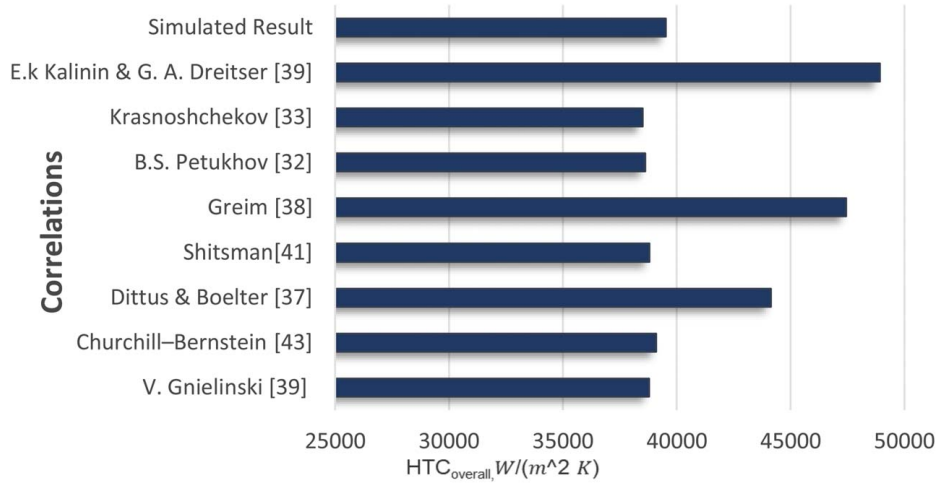

Fig. 6 $HTC_{overall}$ value comparison with simulated value

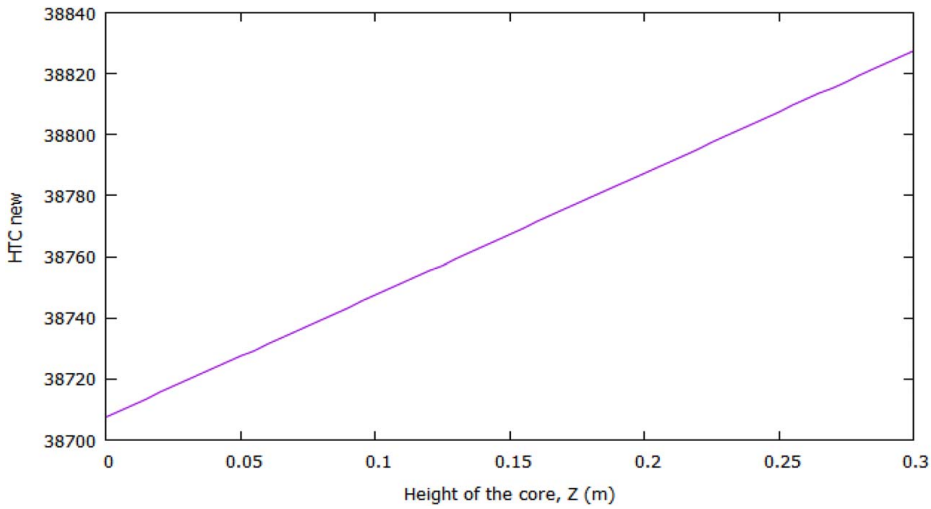

Fig. 7 Graphical demonstration of HTC_{new} along with the height of the core

thermal analysis for all the combinations, U_3Si_2 and U_3Si_5 with AISI 348 can be used in VVER-1200 considering its maximum temperature follows the fuel concept within melting point margin and low hydrogen production.

3.2 Heat Transfer Coefficient. To calculate the referenced HTC_{avg} in Fig. 6, different characterizing data such as conductivity, viscosity, Prandtl, and Reynolds numbers, etc., at each 0.005 cm were identified from NIST Reference Fluid Thermodynamic and Transport Pries Database (REFPROP).

Moreover, the average heat transfer coefficient (HTC_{avg}) for the 30 cm was also computed using STAR CCM+ as 39,800.1 W/m^2K after 103 iterations (Fig. 5). The considerable modal analysis for this iteration is 38,735.81 W/m^2K. Hence, the comparison between simulated and theoretically calculated HTC is indicated in Fig. 6.

Here, the simulated values are very close to all the relations except for those of Dittus and Boelter [37], Greim [38], and Kalinin and Dreitser [39], due to their course of application and geometry and factor consideration which are concisely mentioned in Tables 2 and 3. Furthermore, the reliability interpretation R-squared values of the correlations considering residuals and the analytical results were found as 0.998, which is recommended as in the excellent range [40]. Therefore, the mean HTC value for the same element for these relations can be calculated with 310 data sets to indicate a simple HTC relation and the core height with the prementioned conditions

$$HTC_{new} = 7.8835z^2 + 397.19z + 38{,}708$$

The graphical demonstration by GNUplot is in Fig. 7. A corrective factor, k at the center of the fuel, needs to be identified for further analysis to conclude this research.

4 Conclusions

This study proposed a fuel material and measured thermal response under normal operation. It provides an overview of the lower part efforts underway to support the models to be included in the STAR CCM+ analysis. To summarize the article, the specifics result from these concepts are the following:

- Among all types of U_xSi_x fuels and AISI claddings, U_3Si with any steel cladding is not applicable for reactor operating conditions. The combination of U_3Si_5, U_3Si_2, and AISI-348 is highly capable of reactor applications in the LWRs because of their high heat generation with maximum fuel center

Downloaded from http://risk.asmedigitalcollection.asme.org/openengineering/article-pdf/doi/10.1115/1.4054476/6881352/aoje_1_011023.pdf by guest on 23 June 2024

temperature and an average temperature within the melting point margin. Besides, integrating mechanical and thermal characteristics of U_3Si_2 and AISI-348 placed them as a perfect competitor with conventional fuels.

- The following simple polynomial equation for the HTC has been formulated, with a dependency along with the height for the first half of the reactor and symmetric for the other half

$$\mathrm{HTC}_{new} = 7.8835z^2 + 397.19z + 38{,}708 \pm k$$

The corrective factor k indicates additional neutronic study such as the effect of inherent systems, burnable poison, control rod, fission gas release in U_3Si_5, and irradiation creep in AISI-348, are essential but urge advanced computational facilities for further investigation. However, the equation will be beneficial because of its simplicity during the calculation of the reactor heat transfer analysis for the recommended fuel assembly of VVER-1200.

Acknowledgment

The authors of this paper express their sincere appreciation to the Bangladesh Atomic Energy Commission for arranging the grant for this research, which allows theoretical knowledge to be used in real-world circumstances. The authors would also like to thank the honorable delegates Kirill V. Kutsenko and Demetri Kuzmenkov, as well as the lab facilities of the National Research Nuclear University (NRNU MEPhI), Department of Nuclear Physics and Technologies in Moscow, Russia, and show their gratitude for sharing their pearls of knowledge in this research.

Conflict of Interest

There are no conflicts of interest. This article does not include research in which human participants were involved. Informed consent is not applicable. This article does not include any research in which animal participants were involved.

Data Availability Statement

The data sets generated and supporting the findings of this article are obtainable from the corresponding author upon reasonable request.

Nomenclature

h = enthalpy (J)
D = diameter (mm)
G = mass flow rate, (kg/s)
K = turbulent kinetic energy (J/kg)
L = length
M = molecular mass (kg/kmol)T = temperature (k/°C)
h_{lg} = latent heat of vaporization (kJ/ kg^{-1})
q_o = maximum linear density of heat flux(W/m^2)
C_p = specific heat capacity [kJ/kg]
H_{eff} = effective height of the core
K_r = irregularity coefficient along the core radius
K_z = irregularity coefficient for the height of the core
N_a = the number of fuel assemblies (Pcs.)
Q_c = convection heat flux, W/m^2
R_f = fuel resistance for cladding
R_g = gap thermal resistance
R_{sh} = cladding thermal resistance
S_{ij} = mean flow quantity
T_c = fuel center temperature
T_{sh} = cladding temperature
T_w = fuel surface/periphery temperature
y^+ = dimensionless wall distance
Nu = Nusselt number
Re = Reynolds number
ΔP = pressure drop (MPa)λ = thermal conductivity (W/mK)
μ_{lf} = dynamic viscosity at the fluid temperature (kg/s.m)
μ_{lw} = dynamic viscosity the inner wall surface temperature (kg/s.m)υ = kinematic viscosity (m^2/s)

References

[1] de Souza Gomes, D., Abe, A., e Silva, A. T., Giovedi, C., and Martins, M. R., 2016, "Evaluation of Corrosion on the Fuel Performance of Stainless-Steel Cladding," EPJ Nucl. Sci. Technol., **2**(40), pp. 1–6.
[2] Kalin, B. A., Kalashnikov, A. N., Chernov, I. I., and Shmakov, A. A., 2012, "Hydrogen Problems in Reactor Materials," Proceedings of the 7th International Workshop of Young Scientists and Professionals, Russian Federation, Oct. 24–28, pp. 10–54.
[3] Fuketa, T., Sasajima, H., and Sugiyama, T., 2001, "Behavior of High-Burnup PWR Fuels With Low-Tin Zircaloy-4 Cladding Under Reactivity-Initiated-Accident Conditions," Nucl. Technol., **133**(1), pp. 50–62.
[4] Gamble, K. A., Hales, J. D., Pastore, G., Barani, T., and Pizzocri, D., 2016, "Behavior of U_3Si_2 Fuel and FeCrAl Cladding Under Normal Operating and Accident Reactor Conditions," Environmental Sci.
[5] Massih, A. R., 2018, "UO_2 Fuel Oxidation and Fission Gas Release," Quantum Technologies Report, stralsakerhetsmyndigheten.se.
[6] Goldner, F., 2013, "Overview of Accident Tolerant Fuel Development," OECD/NEA Workshop on Characterization and PIE , DoE, United States.
[7] Bischoff, J., Blanpain, P., Brachet, J.-C., Lorrette, C., Ambard, A., Strumpell, J., and Mckoy, K., "Development of Fuels With Enhanced Accident Tolerance," International Atomic Energy Agency, Nuclear Fuel Cycle, and Materials Section, Vienna (Austria), p. 388.
[8] Burns, P. C., Ewing, R. C., and Navrotsky, A., 2012, "Nuclear Fuel in a Reactor Accident," Science, **335**(6073), pp. 1184–1188.
[9] Allen, T., Busby, J., Meyer, M., and Petti, D., 2010, "Materials Challenges for Nuclear Systems," Mater. Today, **13**(12), pp. 14–23.
[10] White, J. T., Nelson, A. T., Dunwoody, J. T., Byler, D. D., Safarik, D. J., and McClellan, K. J., 2015, "Thermo-physical Properties of U_3Si_2 to 1773K," J. Nucl. Mater., **464**, pp. 275–280.
[11] White, J. T., Nelson, A. T., Byler, D. D., Safarik, D. J., Dunwoody, J. T., and McClellan, K. J., 2015, "Thermo-physical Properties of U_3Si_5 to 1773K," J. Nucl. Mater., **456**, pp. 442–448.
[12] White, J. T., Nelson, A. T., Byler, D. D., Valdez, J. A., and McClellan, K. J., 2014, "Thermo-physical Properties of U_3Si to 1150 K," J. Nucl. Mater., **452**(1–3), pp. 304–310.
[13] Hofman, G. L., 1986, "Crystal Structure Stability and Fission Gas Swelling in Intermetallic Uranium Compound," J. Nucl. Mater., **140**(3), pp. 256–263.
[14] Birtcher, R. C., Richardson, J. W., and Mueller, M. H., 1996, "Amorphization of U_3Si_2 by Ion or Neutron Irradiation," J. Nucl. Mater., **230**(2), pp. 158–163.
[15] Birtcher, R. C., Richardson, J. W., and Mueller, M. H., 1997, "Amorphization of U_3Si by Ion or Neutron Irradiation," J. Nucl. Mater., **244**(3), pp. 251–257.
[16] Finlay, M. R., Hofman, G. L., and Snelgrove, J. L., 2004, "Irradiation Behavior of Uranium Silicide Compounds," J. Nucl. Mater., **325**(2–3), pp. 118–128.
[17] Antonioa, D. J., Shresthaa, K., Harpa, J. M., Adkinsa, C. A., Zhanga, Y., Carmacka, J., and Gofryka, K., 2018, "Thermal and Transport Properties of U_3Si_2," J. Nucl. Mater., **508**, pp. 154–158.
[18] Kim, Y. S., 2012, "Uranium Intermetallic Fuels (U–Al, U–Si, U–Mo)," Compr. Nucl. Mater., **3**, pp. 391–420.
[19] Yao, T., Gong, B., He, L., Miao, Y., Harp, J. M., Tonks, M., and Lian, J., 2018, "In-situ TEM Study of the Ion Irradiation Behavior of U_3Si_2 and U_3Si_5," J. Nucl. Mater., **511**, pp. 56–63.
[20] Bragg-Sitton, S., Todosow, M., Montgomery, R., Stanek, C. R., Mont Gomery, R., and Carmack, W. J., 2016, "Metrics for the Technical Performance Evaluation of Light Water Reactor Accident-Tolerant Fuel," Nucl. Technol., **195**(2), pp. 111–123.
[21] Chen, S., and Yuan, C., 2019, "Minor Actinides Transmutation in Candidate Accident Tolerant Fuel-Claddings U_3Si_2-FeCrAl and U_3Si_2-SiC," Ann. Nucl. Energy, **127**, pp. 204–214.
[22] Harp, J. M., Lessing, P. A., and Hoggan, R. E., 2015, "Uranium Silicide Pellet Fabrication by Powder Metallurgy for Accident Tolerant Fuel Evaluation and Irradiation," J. Nucl. Mater., **466**, pp. 728–738.
[23] Chawla, T. C., Graff, D. L., Borg, R. C., Bordner, G. L., Weber, D. P., and Miller, D., 1981, "Thermophysical Properties of Mix Oxide Fuel and Stainless-Steel Type 316," Nucl. Eng. Des., **67**(1), pp. 57–74.
[24] Abe, A., Giovedi, C., Gomes, D. S., and e Silva, A. T., 2014, "Revisiting Stainless Steel as PWR Fuel Rod Cladding After Fukushima Daiichi Accident," J. Energy Power Eng., **8**, pp. 973–980.
[25] Pino, E. S., Abe, A. Y., and Giovedi, C., 2015, "The Quest For Safe And Reliable Fuel Cladding Materials," Proceedings of the International Nuclear Atlantic Conference—INAC, São Paulo, SP, Brazil.
[26] Beeston, J. M., 1981, "Mechanical and Physical Properties of Irradiated Type 348 Stainless Steel," Effects of Radiation on Materials: 10th Conference, Salt Lake City, UT, Aug. 13–15.
[27] Peckner, D., and Bernstein, I. M., 1977, *Handbook of Stainless Steels*, McGraw-Hill, New York.
[28] Pasupathi, V., 1981, "Investigations of Stainless-Steel Clad Fuel Rod Failures and Fuel Performance in the Connecticut Yankee Reactor," EPRI 2119, Palo Alto, CA.

Downloaded from http://risk.asmedigitalcollection.asme.org/openengineering/article-pdf/doi/10.1115/1.4054476/6881352/aoje_1_011023.pdf by guest on 23 June 2024

[29] Giovedi, C., e Silva, A. T., Abe, A., Gomes, D. S., Cherubini, M., and D'Auria, F., 2014, "Comparison of Fuel Performance Codes Using Stainless Steel as Cladding Material," Proceeding of WRFPM Sendai, Sendai, Japan, Sept. 14–17.
[30] Beeston, J. M., 1980, "Mechanical and Physical Properties of Irradiated Type 348 Stainless Steel," International Symposium on Effects of Radiation on Materials, Savannah, GA.
[31] Strasser, A, and S.M. Stoller Corporation, 1982, *An Evaluation of Stainless-Steel Cladding for Use in Current Design LWRs, NP-2642*, EPRI, California.
[32] Petukhov, B. S., Genin, L. G., Kovalev, S. A., and Solovyev, S. L., 2003, *Heat Transfer in Nuclear Power Plants*, MEI Publisher, Moscow, p. 548.
[33] Krasnoshchekov, E. A., Protopopov, V. S., Kuraeva, I. V., and Antonov, A. M., 1973, ""An Approach to the Determination of the Conditions of Occurrence of Deteriorated Heat Transfer Regimes at Supercritical Pressures (Russian)," High Temp. **11**, pp. 529–532.
[34] Goldberg, I., 1969, "A Procedure For Calculation Of Steady-State Temperature in Zircaloy-Clad, Bulk-Oxide Fuel Elements Using The Figro Computer Program(Lwbr Development Program)," Bettis Atomic Power Laboratory, Pittsburgh, Westinghouse Electric Corporation, WAPD-TM-T5T.
[35] Rahgoshay, M., and Rahmani, Y., 2007, "Study of Temperature Distribution of Fuel, Clad, and Coolant in the VVER-1000 Reactor Core During Group-10 Control Rod Scram by Using Diffusion and Point Kinetic Methods," Nukleonika, **52**(4), pp. 159–165.
[36] Shima, E., Kitamura, K., and Haga, T., 2013, "Green-Gauss/Weighted-Least-Squares Hybrid Gradient Reconstruction for Arbitrary Polyhedra Unstructured Grids," AIAA J, **51**(11), pp. 2740–2747.
[37] Dittus, F. W., and Boelter, L. M. K., 1930, *Heat Transfer in Automobile Radiators of Tubular Type*, Vol. 13, The University of California, Publications of Engineering, California, pp. 443–461.
[38] Griem, H., 1996, "A New Procedure for the Prediction of Forced Convection Heat Transfer at Near- and Supercritical Pressure," Heat Mass Transfer, **31**(2), pp. 301–305.
[39] Kalinin, E. K., and Dreitser, G. A., 1972,"Experimental Investigation of Local Heat Transfer and Hydraulic Resistance With the Cooling of a Gas in a Tube," Teplofizika Vysokikh Temperatur, **8**(6), pp. 1228–1234.
[40] Gnielinski, V., 1975, "New Equations for Heat and Mass Transfer in Pipes and Ducts With a Turbulent Flow," Eng. Res., **41**(1), pp. 8–16.
[41] Shitsman, M. W., 1974, "Heat Transfer to Supercritical Helium, Carbon Dioxide, and Water: Analysis of Thermodynamic and Transport Properties and Experimental Data," Cryogenics, **14**(2), pp. 77–83.
[42] Dwyer, O. E., 1970, *Liquid Metals Handbook, Sodium and Nak Supplement*, U.S. Atomic Energy Commission, Washington, DC, Chap. 5.
[43] Churchill, S. W., and Bernstein, M., 1977, "A Correlating Equation for Forced Convection From Gases and Liquids to a Circular Cylinder in Crossflow," ASME J. Heat Transfer-Trans. ASME, **99**(2), pp. 300–306.

Downloaded from http://risk.asmedigitalcollection.asme.org/openengineering/article-pdf/doi/10.1115/1.4054476/6881352/aoje_1_011023.pdf by guest on 23 June 2024